Transactions of the **13th International Conference on Structural Mechanics in Reactor Technology** (SMiRT 13), Escola de Engenharia - Universidade Federal do Rio Grande do Sul, Porto Alegre, Brazil, August 13-18, 1995

Post-calculation of a feed water pipe break at the Loviisa nuclear power plant

Saarenheimo, A.[1], Eerikäinen, L.[2], Keskinen, R.[3]
1) VTT Manufacturing Technology, Finland
2) VTT Energy, Filand
3) Finnish Centre for Radiation and Nuclear Safety, Finland

ABSTRACT: A dynamic post-calculation is presented for a sudden pipe break which occurred in the main feed water system of the VVER 440 type PWR plant Loviisa 2 on February 25, 1993. A thermal hydraulic code TMOC, based on the method of characteristics, is first used to determine the induced rapid two phase fluid transients. The resulting pressure and momentum flux histories are then applied as an excitation in a nonlinear structural dynamic analysis which makes use of the general purpose finite element code ABAQUS. The permanent relative displacement of the broken pipe ends is finally compared with the value observed after the event. An underestimate of some 30% may for the most part be attributed to scant experimental data and uncertainties in boundary conditions. Assumptions regarding impact against a nearby beam structure and the dynamic stress-strain curve of the ferritic pipe material strongly affect this comparison.

1 INTRODUCTION

A sudden pipe break occurred in the main feed water system of the VVER 440 type PWR plant Loviisa on February 25, 1993. With the plant operating at full power, a start-up of one of the five parallel main feed water pumps was being initiated after an overhaul made for cleaning a strainer on the suction side. The maintenance personnel then observed a leak in a welded connection, shown in Fig. 1, which joins an expansion collar and a flange of a check valve on the discharge side. The leak gradually extended around the pipe circumference until a complete pipe break occurred. The consequent pipe whip phenomenon caused a permanent axial displacement of 560 mm in the vertical pipeline and made the next horizontal pipe portion impact against a nearby beam structure. No injuries were sustained and the leak was safely isolated 9 minutes after the break. The break was attributed to thinning caused by erosion-corrosion. A more detailed description of the event has been given in the NEA Incident Reporting System (NEA/IRS 1993).

This paper deals with a dynamic post-calculation of the incident using general purpose computer codes. The aim was to develop numerical procedures for predicting the damage chains due to breaks of high energy piping not qualifying for the leak-before-break criterion (Wichman et al. 1990). No measured process data are available on the two phase fluid transients during the incident; a thermal hydraulic code TMOC, based on the method of characteristics, was therefore used to determine them theoretically. The resulting pressure and momentum flux histories were applied as an excitation in a nonlinear structural dynamic analysis which made use of the finite element code ABAQUS (Hibbit et al. 1992). The permanent relative displacement of the broken pipe ends was finally compared with the observed value to demonstrate the accuracy which may be expected in practical licencing applications.

2 THERMAL HYDRAULIC MODELLING

The TMOC code was developed at the Technical Research Centre of Finland (VTT) for calculation of fast transients in a two phase flow (Siikonen 1983). Its computational models are defined as a piping network, filled with water and vapour, and consisting of pipes, reservoirs, throttlings and various types of valves and pumps. The code handles abruptly changing phenomena, such as travelling waves in a network, physically correctly without unrealistic damping. To enable accurate description of phase changes, the code includes several models for flashing and condensation rates as a function of the steam void fraction and other governing variables. The code has been benchmarked against several experimental tests and standard problems.

A computational model of 13 pipes and 115 pipe sections as shown in the schema of Fig. 2, was used for the present analysis. It consists of a broken feed water discharge line of length 25 m, inner diameter 289 mm and wall thickness 18 mm, which leads to a T-connection with the main feed water line. The discharge line has two valves, fully open during the incident, and a highly throttling flow meter with orifice of diameter 222 mm. Two physically different parts constitute the model for the main feed water line. The first is a straight pipe of length 15 m. The second part, of length 19.2 m and initial temperature 226° C describes the preheaters and following portion of piping which ends at an infinite reservoir, representing a steam generator. The enthalpy of this reservoir corresponds to a temperature of 242.6° C at pressure 4.69 MPa. All other parts of the piping network are initially subjected to temperature 164° C and internal pressure of ca. 7.0 MPa.

The break occurred at node 1 of the flow model where the expansion collar has a minimum inner diameter of 205 mm, well below that of the discharge line. The breaking hypothesis of Malnes with the Mach number of 0.99 was used to model reaching critical flow conditions at the broken pipe end (Siikonen 1983). The duration of the break was assumed to be 15 ms. Earlier pre-calculations indicate that the exact duration is not very essential as it affects the rate of pressure decrease at the start of discharge only. The flashing (evaporation) model constitutes an other important boundary condition for the analyses. Based on the verification calculations, the Houdayer correlation with constants 0.003 and 4.0 and correction factor 4.2 was employed in the final analysis.

3 FLUID DYNAMIC EXCITATION

The fluid dynamic excitation of the piping originates from the cross-sectional pressure and momentum flux resultants and their differentials at the discontinuities which include the broken pipe end, pipe bends, T-connections, changes of diameter and other minor losses (Keskinen 1981). Within each straight portion, these resultants are in dynamic equilibrium with the forces due to temporal accelerations and density changes of the contained fluid domain. While integration of the latter would yield the excitation as overall forces applied on each straight pipe, the pressure and momentum flux formulation is preferred here as it readily produces a load distribution which physically excites the piping.

Excitation of the discharge line is presented in Fig. 3 in terms of the algebraic sum of the pressure and momentum flux (equivalent pressure) values obtained from thermal hydraulic analysis for five different nodes, defined in Fig. 2. Immediately after the break, the equivalent pressure is seen to decrease rapidly and to fall for a short time below the saturation pressure. The actual pressure falls even further at the break point owing to the critical mass flow rate. Vapour bubbles then start to form, returning the pressure to the saturated state in the piping section preceding the flow meter. The equivalent pressure reaches a value of ca. 1.0 MPa. Downstream of the flow meter, the pressure starts to rise towards the value used as a boundary condition for the steam generator.

During the time period of interest, the flow velocities attained in the discharge line are typically 20 m/s while the jet velocity at the broken pipe end is as high as 40 m/s. The respective mass flow rates are in the range 1000 to 1300 kg/s. The computed equivalent pressures exhibit strong oscillations as the travelling pressure waves are reflected at the pipe ends and throttlings. Continuing the analysis until time 2.2 s would indicate that the oscillations fade out as soon as the warmer water contained in the remote parts of the main feed water line reaches the discharge line and increases the void fraction.

4 STRUCTURAL DYNAMIC ANALYSIS

The finite element model of the discharge line, including 62 pipe and elbow elements, is shown in Fig. 4. The bends of radius of curvature 600 mm were modelled using elbow elements with six circumferential Fourier modes for ovalization, seven integration points through the wall thickness, one integration point in the axial direction and 18 circumferential integration points. Cross-sectional warping was ignored in geometrically nonlinear analysis. The density of steel was modified in all pipe elements to incorporate the mass of the contained liquid water. Valves V1 and V2 of Fig. 2, each having a mass of 978 kg, were modelled with lumped masses located at nodes 15 to 17 and 19 to 21, respectively.

The downstream end of the model is located at the T-connection (node 1) and is treated as fully fixed. This assumption is justified by the greater rigidity of the main feed water line, which has one rigid and one sliding support near the T-connection. The discharge line is additionally supported by three spring hangers S1, S2 and S3, composed of springs and bars joined with hinges. A bilinear spring model, which carries only tension, was used in their finite element analysis. The spring constant of S1 is 630 N/mm and 440 N/mm for both S2 and S3. Whenever the deformation capacity of the springs was exceeded, the slope of the force-displacement curve of the model was taken to match the axial stiffness of the bar.

The lower flange of the horizontal I-beam, located above the topmost horizontal straight portion, was modelled by means of several cylindrical gap elements fixed to the pipe between nodes 40 and 43. The axes of the gap elements were set perpendicular to the pipe axis. Based on the design documentation, the value 250 mm was given to the distance between the gap elements and the outer pipe surface. Since local crushing of the pipe was less than the wall thickness and no measurable deflection was observed in the web of the beam, it was considered reasonable to let the gap cylinder fully constrain the nor-mal velocity component of contacting pipe. Another contact possibly occurred at a hole of diameter 700 mm, made in a concrete floor (level +3.00) for penetration of the long vertical portion of the discharge line. Some spring elements, fixed to nodes 28 and 128, were inserted along the circumference, which was assumed to be concentric with the penetrating pipe cross-section prior to the event.

An elastic-plastic material model with the von Mises yield function and isotropic strain hardening was applied in the analysis. Poisson's ratio was set to 0.3 and a piecewise linear stress-strain curve was defined by the values of Table 1. The effect of the operating temperature 165° C on the CT20 ferritic pipe material was estimated using the stress-strain curves given by a Russian standard (PNAE G-7-002-86 1989).

Table 1. True stress-strain values of the pipe material.

Strain[mm/mm]	0.0019	0.004	0.0218	0.0529	0.1824	0.29
Stress [MPa]	360.0	364.0	379.9	418.2	456.2	460.0

The strain rates during the event were of sufficient magnitude to affect the mechanism

of plastic flow. The ABAQUS code provides a standard procedure for considering the strain rate effects by means of the formula

$$\dot{\varepsilon}_{pl} = D \left[\frac{\tilde{\sigma}}{\sigma^0} - 1 \right]^p \quad (1)$$

where $\dot{\varepsilon}_{pl}$ is the equivalent plastic strain rate, $\tilde{\sigma}$ is the effective yield stress and σ^0 is the static yield stress. For structural steels, the material parameters D and p typically assume the values 40 and 5, respectively. Equation (1) implies an increase in the yield strength, which is well known from experiments on austenitic stainless steels. However, fairly recent results presented by the International Piping Integrity Research Group (Brickstad 1991) suggest that ductile ferritic steels exhibit an opposite phenomenon, known as dynamic strain aging, which instead lowers the ultimate tensile strength at simultaneous high strain rates and temperatures; while the yield strength remains virtually unchanged. Owing to a lack of directly applicable data, results based on Equation (1) and the above material parameter values are presented parallel to those obtained with the static data.

A Rayleigh type damping, proportional to the mass matrix, was introduced in the model to find permanent displacements by direct time integration. The proportionality factor was determined in such a manner that a damping ratio of 5% was achieved for the lowest eigenmodes which dominated elastic vibrations at the broken pipe end (node 55). Damping was speeded up by ignoring the fluid dynamic excitation after time 1 s, whereafter it was too weak to produce plastic deformation.

5 RESULTS

Three dynamic nonlinear analyses were carried out on a Silicon Graphics Crimson workstation using automatic time stepping in direct time integration. The time increments typically assumed values of ca. 10^{-3} s during the applied excitation, whereas during contacts values as small as 10^{-10} s proved necessary. The first analysis (A) was elastic-plastic; the second (B) was elastic-plastic including the strain rate effect; and the third (C) accounted for both the strain rate effect and geometrical nonlinearity.

All displacements are presented in the global coordinate system shown in Fig. 4. The displacement components predicted by analysis A at the break point of the piping are shown in Fig. 5 as a function of time. The maximum value of the vertical displacement (Z direction) is 1.01 m. An approximate value of 0.40 m was estimated for the vertical plastic displacement. The corresponding plastic displacement values for analyses B and C were roughly 200 and 150 mm, respectively. The pipe hits the beam several times in each analysis and gives rise to a maximum contact force of a 3.0 MN.

By the time it impacts with the beam, the pipe has attained a maximum negative displacement in the X direction of nearly 0.5 m. The horizontal displacement of node 35 in the X direction is shown in Fig. 6. A maximum of 0.49 m is attained upon impact. The same result was obtained with analysis B, whereas analysis C yielded a value of 0.46 m. The piping was about to impact with a vertical wall 0.48 m away (see Fig. 2). However, no impact marks were detected. A similar conclusion applies to the downward vertical displacement of node 21, also seen in Fig. 6, since values exceeding 275 mm would have caused the valves to impact with a nearby floor.

According to the geometrically linear analyses A and B, the vertical part of the piping touched the wall at the penetration. The radial displacement at the penetration (node 28) is roughly 190 mm at the most, which equals the distance between the wall and the outer surface of the pipe. However, no evidence of impact was observed.

Each analysis predicted plasticity at the bends and pipe portions which impacted with the beam. The plasticity due to the impact would have a pronounced effect on the vertical displacements of the break point. As the degree of plasticity in turn was particularly sensitive to the strain rate effect, it is evident that analysis A, based on static stress-strain data, would produce the highest permanent displacements of the break point. Underestimation of the measured value by some 30%, even in analysis A, may be attributed mainly to the following factors: 1) uncertainty of the static stress-strain curve; 2) effect of dynamic strain aging on strain hardening; 3) contact phenomena during impacts against the beam; 4) thermal hydraulic assumptions affecting the excitation. These aspects clearly deserve further investigation. However, owing to the significant flexibility of the discharge line during upward motion, the instantaneous maximum displacements probably would have compared much better. This quantity actually governs the effect of pipe whip on plant safety; hence reasonable accuracy is expected in licencing applications.

6 CONCLUSION

The results of this study indicate that existing general purpose thermal hydraulic and elastic-plastic finite element codes are powerful tools for making extensive and realistic pipe whip analyses. The thermal hydraulic analysis was fairly straight-forward, although some uncertainties emerged regarding the boundary conditions and physical modelling. These included the opening time of the break, the formation rate of steam bubbles, and the way of modelling the pipe network beyond the T-connection. However, the results are felt to be reliable over the significant time period of fluid dynamic excitation. Similar conclusions apply to the finite element analysis, which was strongly affected by the applied stress-strain curve and assumptions regarding impacts against nearby structures. Contact-dynamic formulation and material-specific data on strain-rate effects at the operating temperature would certainly improve the results. The experimental data from the real pipe break event analysed in this study were too scant to allow benchmarking of the applied analysis procedures, but indicate that reasonable accuracy may be expected in licencing analyses and other practical applications.

ACKNOWLEDGEMENTS

This study was funded by the Ministry of Trade and Industry, the Technical Research Centre of Finland and the Finnish Centre for Radiation and Nuclear Safety. The assistance of the staff of the Loviisa Nuclear Power Plant is gratefully acknowledged.

REFERENCES

Brickstad, B. 1991. An evaluation of the IPIRG program: SA/FoU-Rapport 91/5. Stockholm: The Swedish Plant Inspectorate (in Swedish).

Hibbit, Karlsson & Sörensen, Inc. 1992. ABAQUS 5.2 User & Theory Manuals.

Keskinen, R. 1981. Hydroelastic Piping Vibration Analysis by Transfer Matrices. Int. J. of Pressure Vessels & Piping 9: 263-283.

NEA/IRS 1993. Feedwater Pipe Rupture at Loviisa 2 Nuclear Power Plant Unit. Report No. 1352.02: Organization for Economic Cooperation and Development.

PNAE G-7-002-86 1989. Strength Analysis Standards for Equipment and Piping at Nuclear Power Plants. Moscow: Energoatomizdat (translation: USNRC 2540).

Siikonen, T. 1983. A Short Description of the Computer Code TMOC: VTT Research Notes 257. Espoo: The Technical Research Centre of Finland.

Wichman, K. & Lee, S. 1990. Development of USNRC Standard Review Plan 3.6.3 for Leak-Before-Break Applications to Nuclear Power Plants. Int. J. of Pressure Vessels & Piping 43: 57-65.

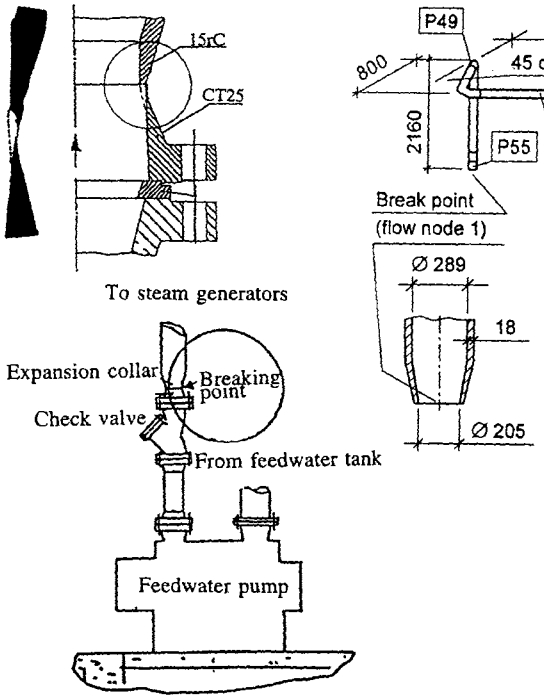

Fig. 1. Location of the pipe break.

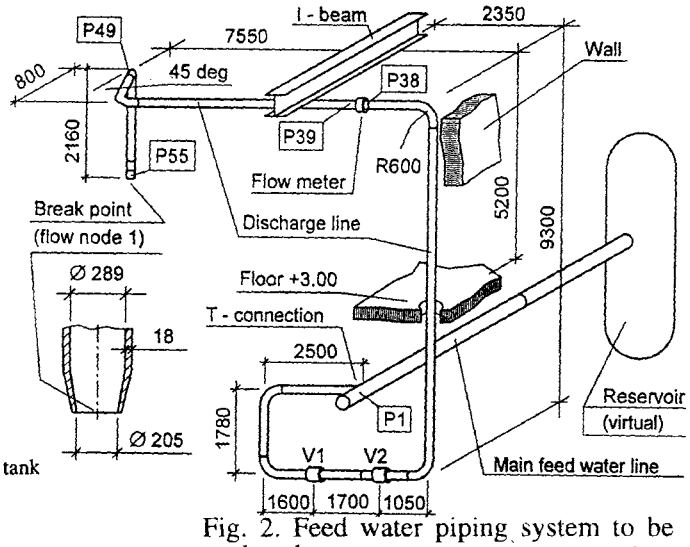

Fig. 2. Feed water piping system to be analysed.

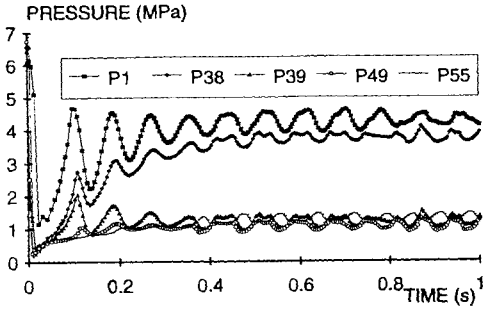

Fig. 3. Equivalent pressure transients at various locations.

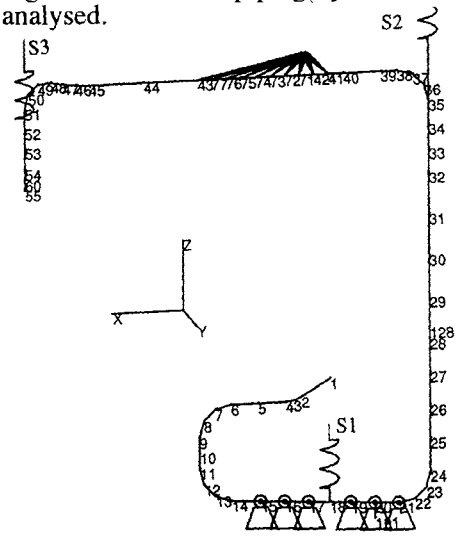

Fig. 4. Finite element model of the discharge line.

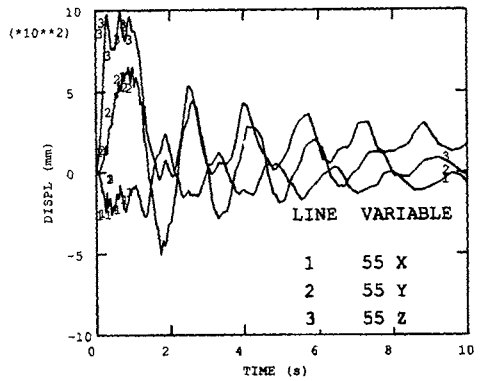

Fig. 5. Displacement components of the break point versus time.

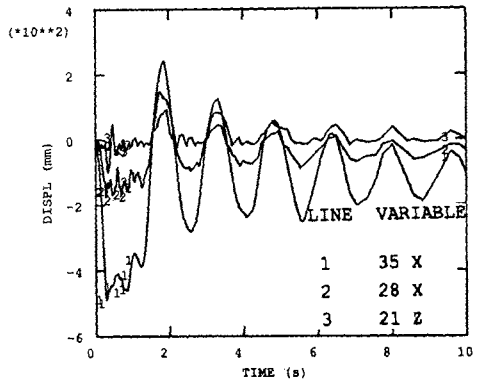

Fig. 6. Displacement components of nodes 21, 28 and 35 versus time.